Molecular Physics
An International Journal at the Interface Between Chemistry and Physics

ISSN: (Print) (Online) Journal homepage: https://www.tandfonline.com/loi/tmph20

Solubility of CO_2 in salty water: adsorption, interfacial tension and salting out effect

S. Blazquez, M. M. Conde & C. Vega

To cite this article: S. Blazquez, M. M. Conde & C. Vega (31 Jan 2024): Solubility of CO_2 in salty water: adsorption, interfacial tension and salting out effect, Molecular Physics, DOI: 10.1080/00268976.2024.2306242

To link to this article: https://doi.org/10.1080/00268976.2024.2306242

MOLECULAR PHYSICS e2306242
https://doi.org/10.1080/00268976.2024.2306242

Taylor & Francis
Taylor & Francis Group

RULL-ABASCAL SPECIAL ISSUE FOR STATISTICAL PHYSICS IN SPAIN (BY INVITATION ONLY)

Solubility of CO_2 in salty water: adsorption, interfacial tension and salting out effect

S. Blazquez [a], M. M. Conde [b] and C. Vega [a]

[a] Dpto. Química Física, Fac. Ciencias Químicas, Universidad Complutense de Madrid, Madrid, Spain; [b] Departamento de Ingeniería Química Industrial y del Medio Ambiente, Escuela Técnica Superior de Ingenieros Industriales, Universidad Politécnica de Madrid, Madrid, Spain

ABSTRACT

In this work, we performed Molecular Dynamics simulations to investigate the solubility of CO_2 in both pure water and NaCl aqueous solutions, employing various force fields for water and NaCl. We first focussed on the solubility of CO_2 in TIP4P/2005 and TIP4P/Ice water models. We found that it was necessary to apply positive deviations to the energetic Lorentz-Berthelot combining rules for the cross interactions of water and CO_2 in both models to accurately replicate the experimental solubility of the gas. Then we found a negative adsorption of ions at the NaCl solution–CO_2 interface. We also observed an increase of the interfacial tensions of the system when adding salt which is related with the observed negative adsorption of the ions at the interface. Furthermore, we found that unit charge models tend to highly overestimate the change in the interfacial tension compared to scaled charge models. Finally, we also explored the salting out effect of CO_2 using different force fields for NaCl. Our findings indicate that unit charge force fields significantly overestimate the salting out effect of CO_2 while the scaled charge model Madrid-2019 accurately reproduces the experimental salting out effect of CO_2 in NaCl solutions.

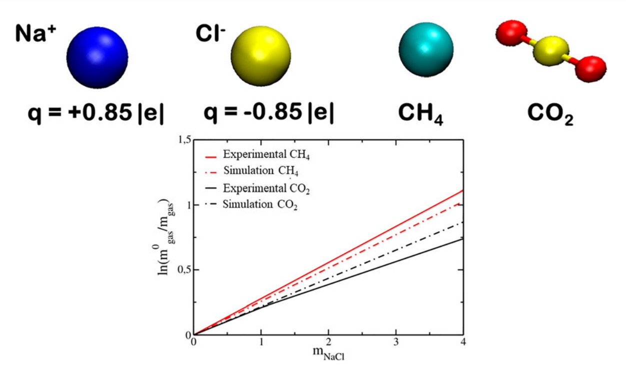

ARTICLE HISTORY
Received 14 November 2023
Accepted 10 January 2024

KEYWORDS
Salting out effect; molecular dynamics simulations; scaled charges; adsorption of ions

1. Introduction

The *salting out* effect refers to the phenomenon where the solubility of a solute in a solvent decreases as the concentration of a salt increases. In this paper we shall consider the particular case in which the solute is in the gas phase (as for instance methane) or in a dense fluid phase (as in the case of carbon dioxide) and we shall refer to the molecules of the solute as the molecules of the gas. The contrary phenomenon is referred to as *salting in* and involves an increase in the solubility of the solute upon the addition of salt. When salts are dissolved in water, they dissociate into ions, creating an ionic environment. This altered environment affects the interactions between the solvent and the solute molecules. In the case of the salting out effect, the presence of ions weakens the interaction between the solute and the water molecules (in the sense of modifying the solvation free energy of the solute to make it less favourable), leading to a decreased solubility of gases in the solution. The study of different gas solubilities in presence of different salts have been experimentally addressed by different authors [1–3]. The salting out effect has also been suggested for the isolation and purification of proteins [4–6]. As a result, there exists significant interest

CONTACT C. Vega ✉ cvega@quim.ucm.es Dpto. Química Física I, Fac. Ciencias Químicas, Universidad Complutense de Madrid, Madrid 28040, Spain

in understanding the interactions between ions and proteins [7–10]. Extensive research has delved into understanding the impact of various salts on the solubility of diverse solutes, primarily to correlate it with the Hofmeister series [9–13]. Moreover, the influence of different salts on the solubility of gases has piqued theoretical interest, leading to simulation-based investigations [14–26].

However, to achieve an accurate depiction of the salting out effect of gases in aqueous solutions, simulations necessitate high-quality force fields for water, gases and salts. In the case of the water and gas force fields we demonstrated in previous works [27] that describing the solubility of methane in water could be achieved by using the TIP4P/2005 force field for water [28] and a simple Lennard-Jones model for methane [29, 30]. However, to obtain agreement with experiments, we had to make modifications to the energetic Lorentz-Berthelot (LB) combining rules [27]. This necessity extends to other gases such as CO_2 [31, 32] and H_2 [33], where the TIP4P/Ice model was employed [34]. Thus, it is evident that when employing a TIP4P-like model and adjusting the LB rules between water and gas, we can accurately describe the solubility of the latter. It is clear that for water the TIP4P/2005 provides excellent results [35] due to the fact that was developed with a carefully selection of target properties and taking into account not only the dipolar but also the quadrupolar moment of water [36, 37]. In fact, Rull and coworkers demonstrated the importance of dipolar and quadrupolar moments in phase equilibria [38–40]. To study the problem of the salting out of gases, in addition to a force field for water and for the gas solute, it is also necessary to introduce a force field for the ions. Although there are a number of force fields for ions, they were not tested in their capacity to reproduce the salting out effect. Moreover, a debate is taking place in the recent years regarding whether to use unit charges (i.e. assigning ions charges of $q = \pm1$) or scaled charges (i.e. assigning ions charges with values lower than ±1).

What is the reason for this debate? In recent years, simulations have become important for tackling problems previously deemed computationally prohibitive. Consequently, when evaluating various properties, it has become evident that many of them are not captured by conventional salt force fields, such as the Joung and Cheatham (JC) model [41] or the Smith and Dang (SD) model [42]. Indeed, these models fall short in reproducing crucial transport properties like viscosity, diffusion coefficient, or electrical conductivity [43–46]. Additionally, these models tend to underestimate salt solubilities when compared to experimental values [44, 47]. Notably, some models, including others apart from the mentioned ones, have even exhibited precipitation and cluster formation phenomena [48–51]. Within this context, Leontyev and Stuchebrukhov [52] introduced a correction that aimed to accurately represent ions in water, involving the assignment of charges of ±0.75 to the ions. Subsequently, Kann and Skinner proposed the use of scaled charges as well, but based on the idea of recovering the Debye–Huckel law [53]. Taking inspiration from these concepts numerous research groups have developed new force fields for salts using scaled charges. In our case, we have also developed a model for a large set of salts by using a charge of ±0.85 and the TIP4P/2005 force field for water. This scaled charge model called Madrid-2019 [54, 55] has proven to be effective in accurately describing various properties, including the temperature of maximum density (TMD) in different electrolyte solutions [56, 57], the freezing temperature depression of ice [58] or the three-phase equilibria of methane hydrates [59].

Nonetheless, scaled charges have recently demonstrated success in describing another interesting property: the salting out effect of methane. In 2007, some of us investigated this problem using a unit charge model, which resulted in an overestimation of the experimental salting out effect [18]. In other words, the simulations predicted lower gas solubilities (more gas expelled from the solution) than what was observed experimentally when salt was added. This problem was revisited in 2020, but employing the Madrid-2019 model featuring scaled charges, we showed a quantitative description of the salting out effect of methane [22]. Thus, revealing that scaled charge models improve the description of salting out effect. In this work, we will undertake a similar investigation using scaled charges, but this time focussing on another intriguing gas: carbon dioxide. The salting out effect of a gas like CO_2 in salty water is a complex phenomenon with important implications for various fields, including environmental science, chemistry and energy production [60–62]. Understanding these interactions is crucial for accurately modelling and predicting the behaviour of gases in saline environments and their impact on natural processes and industrial applications.

2. Simulation details

We have employed the TIP4P/2005 [28] and TIP4P/Ice [34] to model water. Salt has been modelled by using the Madrid-2019 force field [54, 55] which has been developed in combination with the TIP4P/2005 water model. Finally, for CO_2 we have used TraPPe potential [63]. All the parameters of these models are collected in Table 1.

The Lennard-Jones (LJ) parameters for the interactions not collected in Table 1 follow the LB rules except the CO_2–water interactions. These interactions

Table 1. Force field parameters of the water, NaCl and CO_2 models used in this work.

Molecule	q (e)	σ (Å)	ϵ (kJ/mol)
Water			
TIP4P/2005			
O_w	0	3.1589	0.7749
H	0.5564	–	–
M	−1.1128	–	–
TIP4P/Ice			
O_w	0	3.1668	0.88218
H	0.5897	–	–
M	−1.1794	–	–
NaCl			
Na	+0.85	2.21737	1.472356
Cl	−0.85	4.69906	0.076923
Na-Cl		3.00512	1.438894
Na-O_w		2.60838	0.793388
Cl-O_w		4.23867	0.061983
CO_2			
C	0.70	2.8000	0.224478
O	−0.35	3.0500	0.656806

Water molecules are described using the TIP4P/2005 model [28] and TIP4P/Ice [34]. NaCl parameters are those from Madrid-2019 force field [54, 55] and LJ interaction parameters for CO_2 are taken from Ref. [63].

have been obtained by employing the standard Lorentz-Berthelot combining rules for the distances, but the energy parameter was obtained by multiplying by $\chi = 1.11$ the value obtained using default Lorentz-Berthelot energetic combining rules according to Equation (2)

$$\sigma_{ij} = \frac{\sigma_i + \sigma_j}{2} \tag{1}$$

$$\epsilon_{ij} = \chi \sqrt{\epsilon_i \cdot \epsilon_j} \tag{2}$$

When $\chi = 1$, the Lorentz-Berthelot (LB) combining rules are recovered. In this study, as will be discussed in Section 4, we will adjust the CO_2–water interactions by setting $\chi = 1.11$ to achieve a closer match with the experimental solubility of CO_2 in water.

We conducted all simulations using the molecular dynamics GROMACS package version 4.6.5 [64, 65] within the NpT ensemble, maintaining a constant pressure of 200 bar and a temperature of 323.1 K to compare with experimental results. We employed the leap-frog integrator algorithm [66] with a time step of 2 fs. Temperature and pressure were kept constant using the Nosé–Hoover thermostat [67, 68] and the anisotropic Parrinello–Rahman barostat [69] respectively, both with a relaxation time of 2 ps. For van der Waals and electrostatic interactions, a cutoff radius of 0.9 nm was applied. We also incorporated long-range energy and pressure corrections to the Lennard-Jones (LJ) part of the potential (except for the calculations of the surface tension where we used a cutoff of 1.4 nm and did not applied long range corrections to the LJ part of the potential). To account for long-range electrostatic forces, we employed the smooth Particle Mesh Ewald (PME) method [70]. Additionally, the LINCS algorithm [71, 72] was used to maintain the geometry of the water molecules throughout the simulations.

Table 2. Initial number of molecules of the different phases (aqueous NaCl solution and CO_2-rich phase) in the range of concentrations used in this study.

	Number of molecules		
Molality (mol/kg)	Water	NaCl	CO_2
0	6660	0	3000
1	6660	120	3000
3	6660	360	3000

Finally to illustrate the performance of a model with integer charges we shall present some results for the so called JC-TIP4P/2005 [73]. In this force field the Joung and Cheatham force field of NaCl (proposed for SPC/E) [41] is used along the TIP4P/2005 model [28] for water and the interaction between the ions and water is obtained from LB combining rules.

3. Methodology

The salting-out effect is assessed using the empirical Setchenow equation [74]. This equation linearises the natural logarithm of the ratio between the concentration of CO_2 (in moles of CO_2 per kilogram of water) in pure water ($m^0_{CO_2}$) and in a salt solution (m_{CO_2}) with respect to the salt molality, m_{salt} (defined as moles of solute per kg of solvent). The equation is represented as follows:

$$\ln\left(\frac{m^0_{CO_2}}{m_{CO_2}}\right) = k_{salt} m_{salt} \tag{3}$$

where k_{salt} is the salting out coefficient of the Setchenow equation. To calculate the solubility of CO_2 in pure water and in salty water we have performed direct coexistence simulations of pure water or an aqueous NaCl solution and liquid CO_2. We have run 5 independent seeds of 100 ns each one (the first 10 ns are used to equilibrate the system, and the last 90 ns are used as the production period). By analysing the density profiles within the aqueous phase, we can compute the CO_2 concentration in the solution, following the same methodology employed in our prior study on methane [22]. The exact number of molecules employed for this work is collected in Table 2.

4. Results

4.1. Solubility of CO_2 in water

The salting-out effect of a gas is defined as the reduction in the solubility of the gas when salt is added to water. Consequently, the initial step in investigating this phenomenon involves developing a model capable of accurately describing the experimental solubility in pure water (i.e. without the presence of salt). This issue has previously been explored for various gases and water models. For instance, the experimental solubility of methane in water can be faithfully reproduced using the TIP4P/2005 [28] force field for water, a simple LJ model for methane [29, 30], and a positive deviation of a 7% in the energetic LB rule (i.e. $\chi = 1.07$ according to Equation (2)) [27]. Another intriguing example is the behaviour of H_2 gas when modelling in combination with the TIP4P/Ice water model. In this case, achieving a faithful replication of experimental solubility also involves adjusting the interactions between H_2 and water, but notably, the χ factor in this scenario is temperature-dependent [34].

Let us analyse know which would be the optimal value of χ to reproduce the experimental value of the solubility of CO_2 at 200 bar and 323.1 K. To address this problem, we conducted simulations with different values of χ (note that we tuned both interactions, C–O_w and O–O_w). In Figure 1, we show CO_2 solubilities in pure water as a function of the χ factor for both models TIP4P/2005 (red squares) and TIP4P/Ice (blue dots). When we do not apply deviations from the LB rules (i.e. $\chi = 1$), the solubility of CO_2 in water is significantly underestimated, amounting to approximately half of its actual value. It is also evident from the figure that an increase in the χ factor yields to an enhancement in the solubility of CO_2 in water. This relationship between χ and solubility is not linear, although it appears to exhibit some linearity within the range of 1.08 –1.13. Considering the inherent uncertainty in the results, we propose that the optimal value for reproducing the solubility of carbon dioxide in water is $\chi = 1.11$ for both models (which strikingly possess the same trend). Notably, this value closely aligns with the one suggested by Economou and coworkers [32] for the TIP4P/2005, which was $\chi = 1.115$ but differs slightly in the case of TIP4P/Ice, where they proposed a value of $\chi = 1.08$ while we suggest also $\chi = 1.11$. Therefore, from now on, all the results presented in this work correspond to results obtained using χ (or $\chi_{CO_2-H_2O}$) = 1.11 and are the average value of 5 independent simulations. At this point, an intriguing question arises: can the parameter χ effectively reproduce the solubility of CO_2 in water under varying thermodynamic conditions for these two models? In pursuit of an answer, we performed simulations at 200 bar and 284 K, a point that lies on the three-phase experimental coexistence of CO_2 hydrate-water-CO_2. For TIP4P/2005, our simulations yielded a solubility estimate of approximately 1.67 mol/kg, while the experimental value stood at roughly 1.7 mol/kg [75]. Evidently, TIP4P/2005 demonstrates the capability to accurately model CO_2 solubility in water across different thermodynamic conditions when χ is set to 1.11.

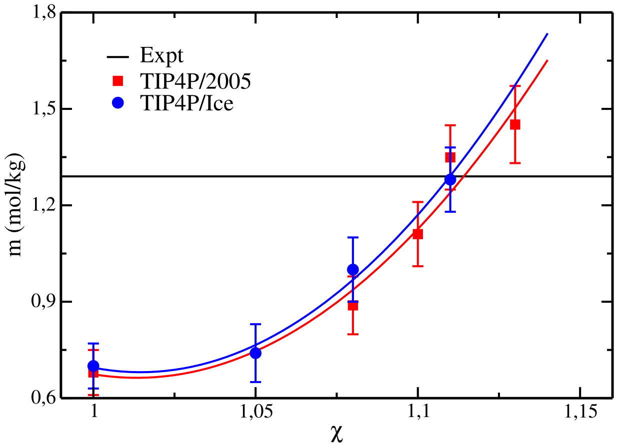

Figure 1. Dependence of the carbon dioxide solubility in water (in molality units) on the deviation factor χ of the energetic LB cross interactions by using the TIP4P/2005 (red squares) and TIP4P/Ice (blue dots) water force fields and the TraPPe model for CO_2. Solid red and blue lines are quadratic fits of their corresponding simulation data and the solid black line is the experimental CO_2 solubility at 200 bar and 323.1 K.

In contrast, TIP4P/Ice, under identical thermodynamic conditions (200 bar and 284 K) and employing the same value of χ (1.11), gives a significantly higher solubility value of 2.26 mol/kg. This result indicates that TIP4P/Ice tends to overestimate the experimental solubility of CO_2 in water in these particular thermodynamic conditions. The reasons behind this different performance can be ascribed to the thermodynamic behaviour of the water models at lower temperatures, specifically involving their temperature of maximum in density (TMD).

In Figure 2, we present the density of pure water at 200 bar as a function of temperature for the TIP4P/2005 and TIP4P/Ice force fields. Both models provide accurate densities at 323 K, the thermodynamic conditions mainly employed in this study. However, a distinct contrast emerges as we delve into lower temperatures. While the TIP4P/2005 model consistently provides accurate density predictions, the TIP4P/Ice model underestimates the experimental densities.

This discrepancy in density predictions holds the key to the divergent behaviours observed in the solubilities of both models. To accurately predict solubilities, it is necessary to correctly describe the density of pure water. In the context of a Widom insertion method [76], when densities are underestimated, it implies that there is more available space for the insertion of molecules, which consequently leads to an overestimation of solubilities.

In our case, at 323 K, both models effectively reproduce the experimental densities, resulting in accurate solubility predictions. However, when we shift our focus to lower temperatures, the TIP4P/2005 model accurately

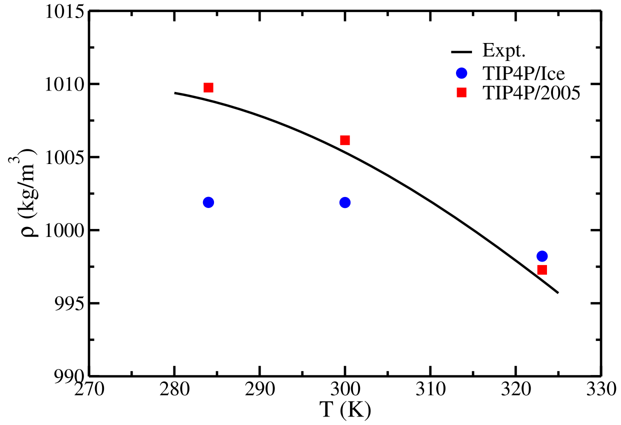

Figure 2. Density of pure water as a function of temperature at 200 bar and using the TIP4P/2005 and TIP4P/Ice force fields.

predicts both the experimental densities and, as a natural consequence, the experimental solubilities. Conversely, the TIP4P/Ice model falls short by underestimating the densities at 284 K, ultimately leading to an overestimation of the experimental solubilities under those specific conditions.

The results for the TIP4P/2005 water model suggests that a constant value of χ in a certain moderate range of T and p should be successful in reproducing the experimental solubilities provided that the model of water used is also able to describe the experimental densities of pure water. The fact that for TIP4P/Ice, the value of $\chi = 1.11$ reproduces correctly the solubility of CO_2 in water at 323.1 K but not at 284 K (along the 200 bar isobar) is rather due to the failure of the model in describing the experimental densities of pure water and not to an error in describing the strength of the water–CO_2 interaction.

Obviously to reproduce the experimental solubility of CO_2 in pure water at 200 bar and 284 K using TIP4P/Ice a smaller value of χ should be used to compensate the error in the density of pure water (and in fact this has been already suggested in previous works [31, 32]).

It is noteworthy that studies on the solubility of CO_2 in water have been conducted employing Drude-type polarisable models for water, specifically the BK3 [77], GCP [78] and HBP [79] models, along with a polarisable Gaussian charge model for CO_2 (as discussed in works by Panagiotopoulos and coworkers) [80, 81]. In these works, they successfully replicated experimental solubilities of carbon dioxide in water. However, it was also necessary to tune the cross interactions between water and CO_2 for accurate reproduction. Additionally, there exist data-driven Many-Body Models for CO_2 developed by Paesani *et al.*, though these models have not been applied yet to calculate CO_2 solubility in water [82, 83]. Finally, a recent contribution by Panagiotopoulos and coworkers introduces a neural network-based model for CO_2 that shows promise [84]. Nonetheless, further research is needed to evaluate the effectiveness of polarisable models in accurately reproducing the solubility of CO_2 in water in the presence of salt (i.e. considering the salting-out effect) since to the best of our knowledge studies involving polarisable models of water, salt and CO_2 have not been presented so far.

Finally, it is important to highlight a detail regarding the equilibrium of CO_2 with its other stable species, namely HCO_3^-. We can roughly estimate the quantities of each species present in the solution. Considering that the acid constant of carbonic acid is $4.7\cdot10^{-7}$ M at standard room temperature and pressure, along with the experimental solubility of CO_2 under the thermodynamic conditions investigated in this study (1.29 mol/kg), we can deduce that approximately 99.94% of the molecules in the solution are composed of CO_2. Consequently, our simulation accurately represents the system with negligible deviations from its true composition.

4.2. Adsorption of ions at the interface

When addressing interfacial systems, it is essential to consider various interfacial phenomena that can take place. In this particular scenario, it is likely that we will observe a phenomenon where ions are adsorbed negatively at the interface. As a result, the molality of the aqueous phase may increase compared to our initially proposed value. To calculate the adsorption of ions and CO_2 at the interface. we will employ the density profiles presented in Figure 3(a–b). The first step in studying adsorption is to set the so-called Gibbs dividing surface for the solvent (water). This surface is the one that gives zero adsorption of water. Once fixed this value, the calculation of the adsorption of any species at the solvent interface can be calculated with the following equation:

$$\Gamma_B = \int_{-\infty}^{z_A} (\rho_B(z) - \rho_{B,H_2O})\,dz + \int_{z_A}^{\infty} (\rho_B(z) - \rho_{B,CO_2})\,dz \qquad (4)$$

where z_A is the position of the Gibbs dividing surface of the water, $\rho_B(z)$ is the number density function of species B along the z-axis and ρ_{B,H_2O} and ρ_{B,CO_2} are the average number densities of B in water and carbon dioxide rich-phases respectively. We calculated the adsorption of ions and carbon dioxide at the interface using Equation (4) and based on the density profiles depicted in Figure 3(a–b). The resulting numerical data are summarised in Table 3. As anticipated, ions exhibit a negative adsorption at the interface, leading to an increase in surface tension as we will explain in the next section. Interestingly, we observe that both ions (Na^+ and Cl^-) exhibit the same adsorption value in all cases (within the error bars), indicating no preferential adsorption of either ion at the interface. In other case, the interface will be partially charged, leading to a lack of electroneutrality in the bulk phase. Furthermore, this ion adsorption is consistent with *in silico* calculations performed by other authors [85–88] for a water-air interface. Various authors have addressed this issue. In 2004, Bhatt *et al.* [85] observed an adsorption close to −0.5 NaCl molecules/nm^2 at concentrations of 2.4 and 4.1 M (although it is worth noting that their calculations had a significant associated error). Subsequently, Santos *et al.* [86] found that, for NaI and KF solutions, ion adsorption at the interface became more negative as the concentration increased. This observation is consistent with the Gibbs equation (see [86] for a detailed discussion):

$$\Gamma \simeq -\frac{c}{RT}\frac{\partial \gamma}{\partial c} \tag{5}$$

In this equation, it can be observed that if γ changes linearly with the salt concentration, the adsorption Γ also changes linearly with the concentration. Subsequently, D'Auria *et al.* [87] also observed negative adsorption for a unit charge model of NaCl, with values of approximately −0.3 molecules/nm^2 at 1.2 M and −0.8 molecules/nm^2 at 6.17 M. Our results are in concurrence with all these computational calculations showing the trend of increasingly negative adsorption with higher salt concentration. Furthermore, our calculated adsorptions of around −0.12 molecules/nm^2 at 1 m and −0.55 molecules/nm^2 at 3 m are in quantitative agreement with those calculations, considering the differences in the system (air-water *vs.* CO_2-water), distinct thermodynamic conditions and various employed models. Indeed, the choice of force field has a substantial impact on adsorption phenomena, as recently demonstrated by Breton and Joly [88]. They found that models with higher charges for ions (i.e. unit charge models) result in more substantial negative adsorptions than scaled charge models with lower ionic charges. This observation aligns with our simulations, where at 3 m the unit charge model JC-TIP4P/2005 yields larger adsorption values (around −0.64 molecules/nm^2) compared to the Madrid-2019 force field (approximately −0.55 molecules/nm^2). Additionally, we find a positive adsorption of CO_2 at the interface, which is consistent across all models. Notably, this positive adsorption is more pronounced in the absence of salt.

It is worth noting that the negative adsorption of ions at the interface results in a bulk molality higher than the one initially proposed as we have previously mentioned. With an average interfacial area of 27.5 nm^2, accounting for two interfaces, and an average adsorption at 3 m of about −0.5 molecules/nm^2, we can estimate a deficit of 27 NaCl molecules transitioning from the interface to the bulk. This leads to a real bulk concentration of approximately 3.2 m (in the case of systems with an initial molality of 3 m), a finding that is consistent with the observations made in the density profiles. Considering these results, all calculations presented in this work, from this point onward, will be reported at the actual concentrations of the solution, accounting for the negative ion adsorption phenomenon. Notice that this is also the case of our previous study with methane (i.e. the actual bulk molalities of that work [22] are slightly larger than the initial ones although this small change was not taken into account in our previous work).

4.3. Interfacial tensions of NaCl aqueous solution-CO_2 system

The negative adsorption of ions previously observed, can be related with an increase in the interfacial tension of the studied system. To connect both properties we have calculated the interfacial tensions of the water-CO_2 system. To tackle this issue, we conducted similar direct coexistence simulations as in the previous section, but with an extended cutoff of 1.4 nm. This adjustment was made because surface tension is a highly sensitive property to the cutoff value [89–91], in contrast to the salting out effect, which, as demonstrated in our prior research [22], remains unaffected by changes in the cutoff value. The interfacial tension of each model can be determined using the following equation:

$$\gamma = \frac{L_z}{2}(p_{zz} - (p_{xx} + p_{yy})/2) \tag{6}$$

where p_{zz} is the normal component of the pressure and p_{yy} and p_{xx} are the tangential components of the pressure (being the z axis perpendicular to the liquid-liquid interface). Notice here that the CO_2 phase is a liquid at these conditions (200 bar and 323.1 K), with a density of about 880 kg/m^3.

The results showing the variation of γ as a function of NaCl concentration at 200 bar and 323.1 K are presented in Figure 4(a), and the numerical data are summarised in Table 4. Notably, the TIP4P/2005 model exhibits a remarkable agreement with the experimental interfacial tension observed in the water-CO_2 interface (27.6 *vs* 29.6 mN/m). Considering that the surface tension of the TIP4P/2005 model for the water-vapour system is 69.3 mN/m at 300 K, as reported by Vega and de Miguel [89], this model effectively captures the substantial reduction in the interfacial tension when in contact with liquid

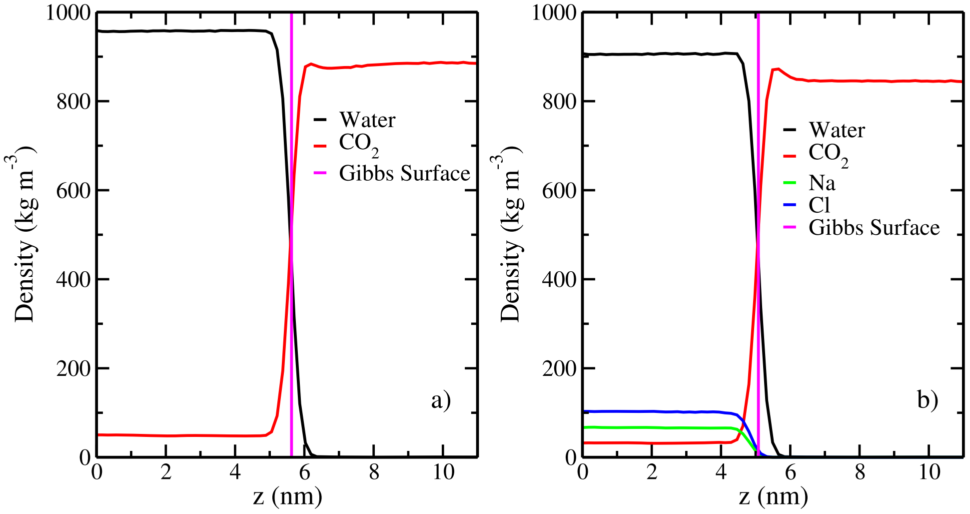

Figure 3. Density profiles of water (black), carbon dioxide (red), sodium (green) and chloride (blue) at 200 bar and 323.1 K. The Gibbs dividing surface is shown in magenta. (a) Water-CO_2 system in absence of salt using the TIP4P/2005 force field. (b) 3 m NaCl aqueous solution-CO_2 using the Madrid-2019 force field.

Table 3. Simulation results for the adsorption of carbon dioxide, Na^+ and Cl^- in aqueous solutions of sodium chloride at 200 bar and 323.1 K (with initial molalities of 1 and 3 m) and using the Madrid-2019 scaled charge model and the JC-TIP4P/2005. As discussed in the main text due to the negative adsorption of NaCl the actual concentrations are slighltly higher than the initial ones.

					Γ_{CO_2}	Γ_{Na}	Γ_{Cl}
Model	Salt	T (K)	p (bar)	m_{NaCl}(mol/kg)		(molecule/nm^2)	
TIP4P/2005	–	323.1	200	0	1.91(08)	0	0
Madrid-2019	NaCl	323.1	200	1.08	0.47(07)	−0.12(01)	−0.13(01)
Madrid-2019				3.20	1.13(07)	−0.52(03)	−0.58(03)
JC-TIP4P/2005	NaCl	323.1	200	3.28	1.01(06)	−0.64(03)	−0.64(03)

Results in the absence of salt for the TIP4P/2005 water model are also presented.

CO_2. It is also evident from our results that the charge of the ions does influence the surface tension, with the unit charge model JC-TIP4P/2005 causing a significant larger increase compared to the scaled charge models.

To gain deeper insights into this effect, we have plotted the variation in interfacial tension (i.e. γ-γ_0, with γ_0 being the interfacial tension of pure water) in Figure 4(b). All the models successfully reproduce the known trend of increasing surface tension when salt is added due to the negative adsorption of ions at the interface. This phenomenon can be readily understood by employing the Gibbs equation (Equation (5)), which shows that a negative adsorption value, denoted as Γ, leads to a positive change in surface tension, represented by γ, as the concentration increases. Additionally, as we observe in Figure 4(a), experimental observations of γ as a function of concentration exhibit a linear upward trend. This trend suggests that within this range, the adsorption value Γ also exhibits a linear increase, albeit in negative values, as the concentration rises.

In Figure 4(b) we also show that the unit charge model JC-TIP4P/2005 highly overestimates the experimental increase in surface tension, whereas the scaled charge model Madrid-2019 exhibits better agreement with the experimental trend. The most significant increase in surface tension observed for the JC-TIP4P/2005 aligns with its more pronounced negative adsorption of ions (-0.64 molecules/nm^2 at 3.28 m) compared to the scaled charge Madrid-2019 (-0.55 molecules/nm^2 at 3.20 m). Surprisingly, the Madrid-2019 model also slightly overestimates the experimental increase in surface tension. This contrasts with our earlier findings [45, 93], where we observed that a charge of ±0.85 underestimated the variation in surface tension for aqueous NaCl solutions-vapour systems. In fact, we recently demonstrated that the optimal charge for reproducing this variation is ±0.92 [45]. However, according to the results presented in this work, it appears that for this system, a charge slightly lower than ±0.85 would be necessary to accurately replicate the experimental trend. These observations emphasise the uniqueness of each system and underscore that findings obtained for the water-vapour system cannot be directly extrapolated to the water-CO_2 system.

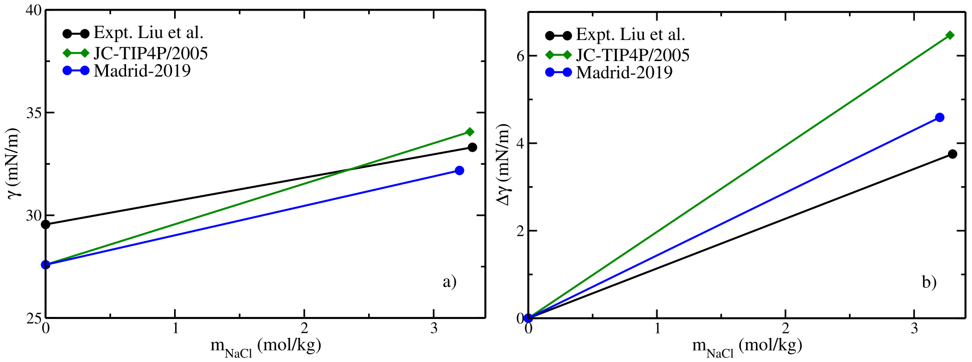

Figure 4. (a) Interfacial free energy at 200 bar and 323.1 K of the carbon dioxide-aqueous NaCl solution as a function of the salt concentration. (b) Variation of the interfacial free energy at 200 bar and 323.1 K of the carbon dioxide-aqueous NaCl solution as a function of the salt concentration. Experimental results have been taken from the work of Liu *et al.* [92]. Solid lines are fit to the experimental and simulation results for: Experiments (black), Madrid-2019 (blue) and JC-TIP4P/2005 (green).

Table 4. Simulation results for the interfacial tensions at 200 bar and 323.1 K of the carbon dioxide-aqueous NaCl solution at different salt concentrations (with initial molality of 3 m) using the Madrid-2019 and the JC-TIP4P/2005 force fields.

					γ (mN/m)	
Model	Salt	T (K)	p (bar)	m_{NaCl} (mol/kg)	Sim.	Exp.
TIP4P/2005	–	323.1	200	0	27.59	29.55
Madrid-2019	NaCl	323.1	200	3.20	33.19	32.97
JC-TIP4P/2005	NaCl	323.1	200	3.28	34.06	33.31

Experimental results are from Liu *et al.* [92].

4.4. Salting out effect of CO_2

Once we have determined the optimum value of χ to achieve the accurate solubility of CO_2 in pure water and evaluated the correct bulk concentration due to the negative adsorption of ions at the interface, the next step is to investigate its salting out effect in salty water. There exists multiple sets of experimental data at 200 bar and 323.1 K found in Refs. [94, 95] which are mutually consistent, as demonstrated in Table 5. In our previous work [22] for the salting out effect of methane we demonstrated that the unit charge models tend to overestimate the experimental trend. We found that the Madrid-2019 model, featuring a charge of ±0.85, could successfully reproduce both qualitatively and quantitatively the salting out effect of methane. However, tackling the salting out effect of CO_2 presents a more challenging endeavour due to its quadrupole nature and significantly higher solubility in water, approximately ten more times than that of methane. Figure 5(a) illustrates our findings regarding the salting out effect of CO_2, utilising different force fields (these results are tabulated in Table 5). Similar to the methane case, unit charge models tend to overestimate the experimental trend, resulting in an excessive expulsion of CO_2 from the solution, as was also shown by Vorholz *et al.* [23]. Conversely, the adoption of a scaled charge model such as the Madrid-2019 model leads to improved results, bringing us closer to replicating the experimental trends.

To compare the salting out effect of methane and carbon dioxide, we present the experimental results for both species in Figure 5(b) as solid lines. Additionally, we provide dashed lines representing linear fits to our simulation results, enforcing an intercept at (0,0) for consistency. It is important to note that for methane, the results are derived from our prior work [22], while for CO_2, we have used the results from this study, in both cases using the Madrid-2019 model.

From this comparative analysis, several key insights emerge. Firstly, we observe that methane experiences a more pronounced salting out effect compared to CO_2. This observation underscores that the salting out effect is not solely dependent on the added salt (recent research by Koga and coworkers [19] highlights the role of ion size in the salting out effect of hydrophobes) but also varies based on the specific gas in question. In fact, it appears that a more soluble molecule like CO_2 exhibits a lesser salting out effect. Secondly, our findings underscore the significance of employing scaled charges in the investigation of such phenomena. As depicted in Figure 5(b), our simulations not only anticipate a more significant salting out effect for methane but also capture the

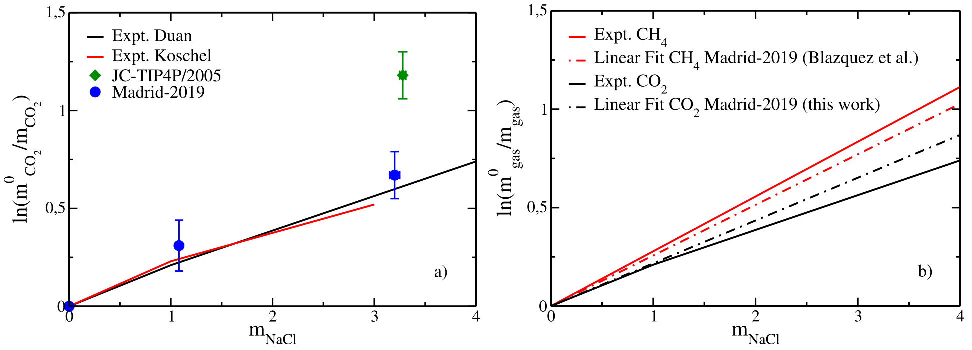

Figure 5. (a) Salting out effect quantified by the natural logarithm of the ratio of the molality of carbon dioxide in pure water ($m^0_{CO_2}$) and in aqueous NaCl solutions (m_{CO_2}), as a function of the molality of NaCl. Results were obtained at 200 bar and 323.1 K. Solid lines are the experimental results obtained from Refs. [94, 95]; green filled diamonds stands for the JC-TIP4P/2005 model and blue filled circles for the Madrid-2019 force field. (b) Comparison between the salting out effect of methane (red) from our previous study [22] and the carbon dioxide (black) calculated in the current work. Experimental results are plotted with solid lines. Dashed lines represent linear fits of the Madrid-2019 force field simulation results with an enforced intercept at (0,0).

Table 5. Simulation results for the salting out of carbon dioxide in an aqueous solution of sodium chloride at 200 bar and 323.1 K with initial molalities of 1 and 3 m and using the Madrid-2019 scaled charge model and the JC-TIP4P/2005 unit charge model.

						$\ln\left(\frac{m^0_{CO_2}}{m_{CO_2}}\right)$		
Model	Salt	T (K)	p (bar)	m_{NaCl} (mol/kg)	m_{CO_2} (mol/kg)	Sim.	Exp. Duan	Exp. Koschel
TIP4P/2005	–	323.1	200	0	1.34	0	0	0
Madrid-2019	NaCl	323.1	200	1.08	0.98	0.31	0.22	0.24
				3.20	0.69	0.67	0.60	0.55
JC-TIP4P/2005	NaCl	323.1	200	3.28	0.41	1.18	0.61	0.56

Results in the absence of salt for the TIP4P/2005 water model are also presented. Experimental results are interpolated from Duan [94] and Koschel [95].

quantitative salting out effect for both gases in alignment with experimental data. This highlights the effectiveness of scaled charge models in providing accurate representations for both gases.

5. Concluding remarks

In this work, we have investigated the solubility of carbon dioxide in water using direct coexistence simulations. Our initial focus was on replicating the experimental solubility of carbon dioxide in pure water. In previous studies [31, 32], there were discrepancies regarding whether it was necessary to introduce deviations to the Lorentz-Berthelot energetic combining rules to achieve agreement with experimental solubility data. Furthermore, if deviations were indeed required, determining the optimal value for these deviations remained an open question. To afford these problems, we have employed the TraPPe model for CO_2 in combination with the TIP4P/2005 and TIP4P/Ice water models. By varying the factor χ in the LB energetic rules (as shown in Equation (2)), we found that a factor of $\chi = 1.11$ was necessary to accurately reproduce the solubility of carbon dioxide under the specific conditions of temperature and pressure and system size employed for both TIP4P/2005 and TIP4P/Ice water models. However, TIP4P/2005 accurately described the solubility in different thermodynamics conditions. Contrary, the TIP4P/Ice was not able to provide an accurate value of the solubility at lower temperatures due to its worse prediction of the TMD.

Subsequently, we investigated the negative adsorption of ions at the interface and we linked it with the impact of salt on the surface tension of aqueous NaCl solutions in contact with a liquid CO_2 phase. Interestingly, all models exhibited an overestimation of the experimental interfacial tension of the system. Notably, the model that displayed the most significant overestimation (the unit charge JC-TIP4P/2005 force field) also presented the largest negative adsorption of ions at the interface. It is worth mentioning that the Madrid-2019 force field has exhibited a negative adsorption of approximately -0.5 molecules/nm^2 at 3 m for the water-CO_2 coexistence, a result consistent with findings in other simulation works [85–88] for the water-air system.

Finally, we encountered the problem of the salting out effect of CO_2 in NaCl solutions, akin to what we observed in the case of methane [22]. It became evident that unit charge force fields tended to significantly overestimate this effect [22, 23]. In order to quantitatively match the experimental trend, we employed the scaled charge model Madrid-2019. We found an excellent agreement with experimental results in this context.

In conclusion, this work contributes to the understanding of the impact of unit charge and scaled charge models on various properties of aqueous NaCl solutions in coexistence with a CO_2 phase. Our results demonstrate that for problems related to the solubility of CO_2 in seawater, the combination of TIP4P/2005, TraPPe and Madrid-2019 models represents an excellent choice. This is again another property where the use of scaled charges for the electrolyte force field improve the results obtained by models using integer charges.

Acknowledgments

We would like to dedicate this work to Prof. Jose Luis Fernandez Abascal (affectionately known as JL among his friends and colleagues). S. B. thanks to JL because he was invaded by his passion as a physical chemistry professor and impelled him to start a scientific career in molecular simulation. M.M.C. extends her profound gratitude to JL for his support throughout her scientific journey. His guidance in maintaining a harmonious balance between academic and personal life has been a valuable lesson. C.V. would like to thank Prof. Abascal for being an example: his curiosity, his rigorous work (error bars included), his intuition, his modesty and his personality was a nice cocktail that made working with him an enjoyable adventure that lasted 25 years. Difficult not to miss the discussions at night via email, the submission of the runs, the lunches together, and his friendship and advice along all these years. JL has shared with all of us his remarkable kindness and his more than demonstrated scientific excellence. We dedicate this work to him with gratitude and admiration for his teaching and research endeavours. One of us (C.V.) would also like to dedicate this paper to the memory of Luis Rull. His enthusiasm about science and about life was enduring his entire life, bringing Seville to the map of Statistical Mechanics in the world and being present in different important events of my life including professional ones (in my PhD defense as an evaluator) or personal ones (the day of my wedding with my wife, Carmen). His influence is still alive in the next generation working on Statistical Physics in Spain. The same is true for others as Santiago Lago (Phd advisor of C. Vega) that assumed the difficult task of elevating the scientific level of Spain from almost a desert (during the 40 years that followed the Spanish civil war) to a flowered garden in the last twenty years with a number of successful scientists and groups all around the country. Manuel Lombardero (PhD advisor of both Abascal and Lago) was the grandfather in Madrid of this school that is still alive. We would like to dedicate this paper to all these people that did the first steps in bringing back Spain in the map of statistical physics all around the world.

Disclosure statement

No potential conflict of interest was reported by the author(s).

Funding

This work was funded by Grants No. PID2022-136919NB-C31 and PID2022-136919NB-C32 of the MICINN. M.M.C. acknowledges CAM and UPM for financial support of this work through the CavItieS project No. APOYO-JOVENES-01HQ1S-129-B5E4MM from ‘Accion financiada por la Comunidad de Madrid en el marco del Convenio Plurianual con la Universidad Politecnica de Madrid en la linea de actuacion estimulo a la investigacion de jovenes doctores’ and CAM under the Multiannual Agreement with UPM in the line Excellence Programme for University Professors, in the context of the V PRICIT (Regional Programme of Research and Technological Innovation). The authors gratefully acknowledge the Universidad Politecnica de Madrid (www.upm.es) for providing computing resources on Magerit Supercomputer. We acknowledge Prof. F. Gamez for helpful discussions.

ORCID

S. Blazquez http://orcid.org/0000-0002-6218-3880
M. M. Conde http://orcid.org/0000-0003-2822-9141
C. Vega http://orcid.org/0000-0002-2417-9645

References

[1] F. Long and W. McDevit, Chem. Rev. **51** (1), 119–169 (1952). doi:10.1021/cr60158a004
[2] H.L. Clever, J. Chem. Eng. Data **28** (3), 340–343 (1983). doi:10.1021/je00033a018
[3] A. Schumpe, Chem. Eng. Sci. **48** (1), 153–158 (1993). doi:10.1016/0009-2509(93)80291-W
[4] K.C. Duong-Ly and S.B. Gabelli, in *Methods in Enzymology*, vol. 541 (Elsevier, 2014), pp. 85–94.
[5] J. Porath, Biopolymers: Original Res. Biomol. **26** (S0), S193–S204 (1987). doi:10.1002/(ISSN)1097-0282
[6] Y.Q. Tang and N. Weng, Bioanalysis **5** (12), 1583–1598 (2013). doi:10.4155/bio.13.117
[7] T. Arakawa and S.N. Timasheff, Biochemistry **23** (25), 5912–5923 (1984). doi:10.1021/bi00320a004
[8] C. Coen, H. Blanch and J.M. Prausnitz, AIChE J. **41** (4), 996–1004 (1995). doi:10.1002/aic.v41:4
[9] R.L. Baldwin, Biophys. J. **71** (4), 2056–2063 (1996). doi:10.1016/S0006-3495(96)79404-3
[10] H.-X. Zhou, Proteins: Struct. Funct. Bioinform. **61** (1), 69–78 (2005). doi:10.1002/prot.v61:1
[11] A.M. Hyde, S.L. Zultanski, J.H. Waldman, Y.-L. Zhong, M. Shevlin and F. Peng, Org. Process. Res. Dev. **21** (9), 1355–1370 (2017). doi:10.1021/acs.oprd.7b00197
[12] P. Jungwirth and P.S. Cremer, Nat. Chem. **6** (4), 261–263 (2014). doi:10.1038/nchem.1899
[13] Y. Zhang and P.S. Cremer, Curr. Opin. Chem. Biol. **10** (6), 658–663 (2006). doi:10.1016/j.cbpa.2006.09.020
[14] M. Kinoshita and F. Hirata, J. Chem. Phys. **106** (12), 5202–5215 (1997). doi:10.1063/1.473519
[15] P.E. Smith, J. Phys. Chem. B **103** (3), 525–534 (1999). doi:10.1021/jp983303c
[16] A. Kalra, N. Tugcu, S.M. Cramer and S. Garde, J. Phys. Chem. B **105** (27), 6380–6386 (2001). doi:10.1021/jp010568+
[17] A.S. Thomas and A.H. Elcock, J. Am. Chem. Soc. **129** (48), 14887–14898 (2007). doi:10.1021/ja073097z
[18] H. Docherty, A. Galindo, E. Sanz and C. Vega, J. Phys. Chem. B **111** (30), 8993–9000 (2007). doi:10.1021/jp0678249
[19] H. Katsuto, R. Okamoto, T. Sumi and K. Koga, J. Phys. Chem. B **125** (23), 6296–6305 (2021). doi:10.1021/acs.jpcb.1c03388

[20] T.A. Ho and A. Ilgen, J. Phys. Chem. B **121** (51), 11485–11491 (2017). doi:10.1021/acs.jpcb.7b09215

[21] G. Graziano, J. Chem. Phys. **129** (8), (2008). doi:10.1063/1.2972979

[22] S. Blazquez, I.M. Zeron, M.M. Conde, J.L.F. Abascal and C. Vega, Fluid Phase Equilib. **513**, 112548 (2020). doi:10.1016/j.fluid.2020.112548

[23] J. Vorholz, V. Harismiadis, A.Z. Panagiotopoulos, B. Rumpf and G. Maurer, Fluid Phase Equilib.**226**, 237–250 (2004). doi:10.1016/j.fluid.2004.09.009

[24] J. Vorholz and G. Maurer, Phys. Chem. Chem. Phys. **10** (48), 7247–7256 (2008). doi:10.1039/b810728a

[25] L.M. Hamm, I.C. Bourg, A.F. Wallace and B. Rotenberg, Rev. Mineral. Geochem. **77** (1), 189–228 (2013). doi:10.2138/rmg.2013.77.6

[26] K. Saadallah, V. Lachet, B. Creton, M.-C. Caumon, A. Randi and J. Sterpenich, Fluid Phase Equilib.**574**, 113901 (2023). doi:10.1016/j.fluid.2023.113901

[27] H. Docherty, A. Galindo, C. Vega and E. Sanz, J. Chem. Phys. **125** (7), 074510 (2006). doi:10.1063/1.2335450

[28] J.L.F. Abascal and C. Vega, J. Chem. Phys. **123**, 234505 (2005). doi:10.1063/1.2121687

[29] B. Guillot and Y. Guissani, J. Chem. Phys. **99**, 8075 (1993). doi:10.1063/1.465634

[30] D. Paschek, J. Chem. Phys. **120**, 6674 (2004). doi:10.1063/1.1652015

[31] J.M. Miguez, M.M. Conde, J.P. Torre, F.J. Blas, M.M. Pineiro and C. Vega, J. Chem. Phys. **142**, 124505 (2015). doi:10.1063/1.4916119

[32] J. Costandy, V.K. Michalis, I.N. Tsimpanogiannis, A.K. Stubos and I.G. Economou, J. Chem. Phys.**143** (9), 094506 (2015). doi:10.1063/1.4929805

[33] V.K. Michalis, I.G. Economou, A.K. Stubos and I.N. Tsimpanogiannis, J. Chem. Phys. **157** (15), 154501 (2022). doi:10.1063/5.0108738

[34] J.L.F. Abascal, E. Sanz, R.G. Fernandez and C. Vega, J. Chem. Phys. **122**, 234511 (2005). doi:10.1063/1.1931662

[35] C. Vega and J.L. Abascal, Phys. Chem. Chem. Phys. **13** (44), 19663–19688 (2011). doi:10.1039/c1cp22168j

[36] J.L. Abascal and C. Vega, J. Phys. Chem. C **111** (43), 15811–15822 (2007). doi:10.1021/jp074418w

[37] J.L. Abascal and C. Vega, Phys. Rev. Lett. **98** (23), 237801 (2007). doi:10.1103/PhysRevLett.98.237801

[38] B. Garzón, S. Lago, C. Vega, E.D. Miguel and L.F. Rull, J. Chem. Phys. **101** (5), 4166–4176 (1994). doi:10.1063/1.467467

[39] B. Garzón, S. Lago, C. Vega and L.F. Rull, J. Chem. Phys. **102** (18), 7204–7215 (1995). doi:10.1063/1.469115

[40] M. Houssa, L.F. Rull and S.C. McGrother, J. Chem. Phys. **109** (21), 9529–9542 (1998). doi:10.1063/1.477615

[41] I.S. Joung and T.E. Cheatham III, J. Phys. Chem. B **112** (30), 9020–9041 (2008). doi:10.1021/jp8001614

[42] D.E. Smith and L.X. Dang, J. Chem. Phys. **100** (5), 3757–3766 (1994). doi:10.1063/1.466363

[43] S. Yue and A.Z. Panagiotopoulos, Mol. Phys. **117** (23-24), 3538–3549 (2019). doi:10.1080/00268976.2019.1645901

[44] A.Z. Panagiotopoulos, J. Chem. Phys. **153** (1), 010903 (2020). doi:10.1063/5.0012102

[45] S. Blazquez, M. Conde and C. Vega, J. Chem. Phys. **158** (5), 054505 (2023). doi:10.1063/5.0136498

[46] S. Blazquez, J.L. Abascal, J. Lagerweij, P. Habibi, P. Dey, T.J. Vlugt, O.A. Moultos and C. Vega, J. Chem. Theory Comput. **19** (16), 5380–5393 (2023). doi:10.1021/acs.jctc.3c00562

[47] J. Espinosa, J. Young, H. Jiang, D. Gupta, C. Vega, E. Sanz, P.G. Debenedetti and A.Z. Panagiotopoulos, J. Chem. Phys. **145** (15), 154111 (2016). doi:10.1063/1.4964725

[48] A.K. Giri and E. Spohr, J. Mol. Liq. **228**, 63–70 (2017). doi:10.1016/j.molliq.2016.09.089

[49] F. Moučka, I. Nezbeda and W.R. Smith, J. Chem. Phys. **138** (15), 154102 (2013). doi:10.1063/1.4801322

[50] E. Wernersson and P. Jungwirth, J. Chem. Theory Comput. **6** (10), 3233–3240 (2010). doi:10.1021/ct100465g

[51] T. Martinek, E. Duboué-Dijon, Š. Timr, P.E. Mason, K. Baxová, H.E. Fischer, B. Schmidt, E. Pluhařová and P. Jungwirth, J. Chem. Phys. **148** (22), 222813 (2018). doi:10.1063/1.5006779

[52] I. Leontyev and A. Stuchebrukhov, J. Chem. Phys. **130** (8), 02B609 (2009).

[53] Z. Kann and J. Skinner, J. Chem. Phys. **141** (10), 104507 (2014). doi:10.1063/1.4894500

[54] I.M. Zeron, J.L.F. Abascal and C. Vega, J. Chem. Phys. **151**, 134504 (2019). doi:10.1063/1.5121392

[55] S. Blazquez, M.M. Conde, J.L.F. Abascal and C. Vega, J. Chem. Phys. **156**, 044505 (2022). doi:10.1063/5.0077716

[56] L. Sedano, S. Blazquez, E.G. Noya, C. Vega and J. Troncoso, J. Chem. Phys. **156** (15), 154502 (2022). doi:10.1063/5.0087679

[57] F. Gámez, L. Sedano, S. Blazquez, J. Troncoso and C. Vega, J. Mol. Liq. **377**, 121433 (2023). doi:10.1016/j.molliq.2023.121433

[58] C.P. Lamas, C. Vega and E.G. Noya, J. Chem. Phys. **156** (13), 134503 (2022). doi:10.1063/5.0085051

[59] S. Blazquez, C. Vega and M. Conde, J. Mol. Liq. **383**, 122031 (2023). doi:10.1016/j.molliq.2023.122031

[60] Z. Tu, P. Liu, X. Zhang, M. Shi, Z. Zhang, S. Luo, L. Zhang, Y. Wu and X. Hu, Sep. Purif. Technol.**254**, 117621 (2021). doi:10.1016/j.seppur.2020.117621

[61] L. Zhang and R. Wang, RSC Adv. **2** (25), 9551–9554 (2012). doi:10.1039/c2ra20882b

[62] V. Muñoz-Iglesias, L.J. Bonales, D. Santamaría-Pérez, M. Taravillo, V.G. Baonza and O. Prieto-Ballesteros, Spectrosc Lett. **45** (6), 407–412 (2012). doi:10.1080/00387010.2011.615879

[63] J.J. Potoff and J.I. Siepmann, AIChE J. **47**, 1676 (2001). doi:10.1002/aic.v47:7

[64] D. van der Spoel, E. Lindahl, B. Hess, G. Groenhof, A.E. Mark and H.J.C. Berendsen, J. Comput. Chem. **26**, 1701 (2005). doi:10.1002/jcc.v26:16

[65] B. Hess, C. Kutzner, D. van der Spoel and E. Lindahl, J. Chem. Theory Comput. **4**, 435–447 (2008). doi:10.1021/ct700301q

[66] D. Beeman, J. Comput. Phys. **20** (2), 130–139 (1976). doi:10.1016/0021-9991(76)90059-0

[67] S. Nosé, Mol. Phys. **52** (2), 255–268 (1984). doi:10.1080/00268978400101201

[68] W.G. Hoover, Phys. Rev. A **31**, 1695–1697 (1985). doi:10.1103/PhysRevA.31.1695

[69] M. Parrinello and A. Rahman, J. App. Phys. **52**, 7182–7190 (1981). doi:10.1063/1.328693

[70] U. Essmann, L. Perera, M.L. Berkowitz, T. Darden, H. Lee and L.G. Pedersen, J. Chem. Phys. **103**, 8577–8593 (1995). doi:10.1063/1.470117

[71] B. Hess, H. Bekker, H.J.C. Berendsen and J.G.E. M. Fraaije, J. Comput. Chem. **18**, 1463 (1997). doi:10.1002/(ISSN)1096-987X

[72] B. Hess, J. Chem. Theory Comput. **4**, 116–122 (2008). doi:10.1021/ct700200b

[73] A.L. Benavides, J.L. Aragones and C. Vega, J. Chem. Phys. **144** (12), 124504 (2016). doi:10.1063/1.4943780

[74] J.M. Prausnitz, R.N. Lichtenthaler and E.G. de Azevedo, *Molecular Thermodynamics of Fluid Phase Equilibria* (Prentice Hall, White Plains, 1999).

[75] L.W. Diamond and N.N. Akinfiev, Fluid Phase Equilib. **208** (1-2), 265–290 (2003). doi:10.1016/S0378-3812(03)00041-4

[76] B. Widom, J. Chem. Phys. **39** (11), 2808–2812 (1963). doi:10.1063/1.1734110

[77] P.T. Kiss and A. Baranyai, J. Chem. Phys. **138** (20), 204507 (2013). doi:10.1063/1.4807600

[78] P. Paricaud, M. Předota, A.A. Chialvo and P.T. Cummings, J. Chem. Phys. **122** (24), 244511 (2005). doi:10.1063/1.1940033

[79] H. Jiang, O.A. Moultos, I.G. Economou and A.Z. Panagiotopoulos, J. Phys. Chem. B **120** (48), 12358–12370 (2016). doi:10.1021/acs.jpcb.6b08205

[80] H. Jiang, O.A. Moultos, I.G. Economou and A.Z. Panagiotopoulos, J. Phys. Chem. B **120** (5), 984–994 (2016). doi:10.1021/acs.jpcb.5b11701

[81] H. Jiang, I.G. Economou and A.Z. Panagiotopoulos, J. Phys. Chem. B **121** (6), 1386–1395 (2017). doi:10.1021/acs.jpcb.6b12791

[82] M. Riera, E.P. Yeh and F. Paesani, J. Chem. Theory Comput. **16** (4), 2246–2257 (2020). doi:10.1021/acs.jctc.9b01175

[83] S. Yue, M. Riera, R. Ghosh, A.Z. Panagiotopoulos and F. Paesani, J. Chem. Phys. **156** (10), 104503 (2022). doi:10.1063/5.0080061

[84] R. Mathur, M.C. Muniz, S. Yue, R. Car and A.Z. Panagiotopoulos, J. Phys. Chem. B **127** (20)), 4562–4569 (2023). doi:10.1021/acs.jpcb.3c00610

[85] D. Bhatt, R. Chee, J. Newman and C. Radke, Curr. Opin. Colloid Interface Sci. **9** (1-2), 145–148 (2004). doi:10.1016/j.cocis.2004.05.020

[86] D.J. dos Santos, F. Muller-Plathe and V.C. Weiss, J. Phys. Chem. C **112** (49), 19431–19442 (2008). doi:10.1021/jp804811u

[87] R. D'Auria and D.J. Tobias, J. Phys. Chem. A **113** (26), 7286–7293 (2009). doi:10.1021/jp810488p

[88] G. Le Breton and L. Joly, J. Chem. Phys. **152** (24), 241102 (2020). doi:10.1063/5.0011058

[89] C. Vega and E. de Miguel, J. Chem. Phys. **126** (15), 154707 (2007). doi:10.1063/1.2715577

[90] F.J. Blas, L.G. MacDowell, E. de Miguel and G. Jackson, J. Chem. Phys. **129** (14), 144703 (2008). doi:10.1063/1.2989115

[91] L.G. MacDowell and F.J. Blas, J. Chem. Phys. **131** (7), 074705 (2009). doi:10.1063/1.3197009

[92] Y. Liu, H.A. Li and R. Okuno, Ind. Eng. Chem. Res. **55** (48), 12358–12375 (2016). doi:10.1021/acs.iecr.6b02446

[93] A.L. Benavides, M.A. Portillo, V.C. Chamorro, J.R. Espinosa, J.L.F. Abascal and C. Vega, J. Chem. Phys. **147** (10), 104501 (2017). doi:10.1063/1.5001190

[94] Z. Duan and R. Sun, Chem. Geol. **193** (3-4), 257–271 (2003). doi:10.1016/S0009-2541(02)00263-2

[95] D. Koschel, J.-Y. Coxam, L. Rodier and V. Majer, Fluid Phase Equilib. **247** (1-2), 107–120 (2006). doi:10.1016/j.fluid.2006.06.006